Analyst

ROYAL SOCIETY OF CHEMISTRY

PAPER

View Article Online
View Journal | View Issue

Cite this: *Analyst*, 2025, **150**, 3643

Identification of representative compounds for saturate, aromatic, resin, and asphaltene (SARA) fractions using the SARA-HPLC technique

Shadi Kheirollahi,[a] Mabkhot BinDahbag,[a] Zahra Abbasi*[b] and Hassan Hassanzadeh *[a]

Petroleum is a complex mixture comprising a diverse range of hydrocarbons. Due to this complexity and the limited knowledge of their chemical structures, identifying representative compounds for their compositional group analysis remains unexplored. In this work, we identified and introduced standard hydrocarbon compounds with characteristics of petroleum fractions—saturates, aromatics, resins, and asphaltenes (SARA)—using the SARA-HPLC analytical technique. The proposed standard SARA compounds exhibit similar behavior to their respective fractions. The proposed saturate standard is a mixture of 67% *n*-C_6 and 33% *n*-C_{36} (wt%), while the aromatic standard includes 65% nitrobenzene and 35% phenanthrene (wt%). The resin standard is composed of 71% anthrone and 29% 9-anthracenemethanol (wt%), and the asphaltene standard contains 62% salicylic acid and 38% bathophenanthroline (wt%). These compounds are adsorbed exclusively onto their corresponding columns in the SARA-HPLC system without any interaction or affinity with other columns, which is highly favorable for SARA fractionation. These proposed standard compounds align with the characteristics of the actual petroleum mixture SARA fractions, demonstrating their accuracy and reliability as representative standards. Additionally, the proposed SARA standards eliminate the need for time-consuming and laborious calibration procedures and references currently used in the petroleum industry while reducing the repeatability and uncertainty challenges caused by current practices in SARA fraction determination.

Received 31st March 2025,
Accepted 1st July 2025

DOI: 10.1039/d5an00367a

rsc.li/analyst

1. Introduction

Crude oil and bitumen are complex mixtures of hydrocarbons with molecular weights ranging from 16 to 3000 atomic mass units, incorporating heteroatoms such as nitrogen (N), sulfur (S), and oxygen (O), as well as trace metals.[1–3] Due to the existence of tens of thousands of species with a broad range of chemical structures, sizes, and polarities within petroleum, it is practically impossible to fully characterize and identify their exact molecular structures and individual physicochemical behaviours.[4,5] To gain insight into their properties, it is common practice to separate petroleum products into four polarity-based fractions: saturates, aromatics, resins, and asphaltenes, referred to as SARA fractions.[4,6,7] Details of fractionation techniques can be found elsewhere.[8] However, the inherent complexity of crude oil and the changing stability of chemical forms make it challenging to precisely identify individual molecular forms of elements.[9] To better understand the chemical behavior of SARA fractions, it is essential to investigate and identify the molecular composition of each fraction.

The saturate fraction comprises nonpolar components with relatively simple molecular structures, while resins and asphaltenes contain numerous complex unsaturated aromatic compounds and polar functional groups. Saturated hydrocarbons primarily consist of straight-chain alkanes ranging from methane (CH_4) with a single carbon atom to larger molecules containing 40 or more carbon atoms, along with branched chains, with the general formula C_nH_{2n+2}, and cyclic structures, known as cycloalkanes or naphthenes.[1,2,10]

The simplest aromatic fraction consists of hydrocarbons with a single aromatic ring (*i.e.*, benzene or C_6H_6), which generally links to linear, branched, or cyclic alkyl substituents, exhibiting slightly more polarity than the saturate fraction. More complex aromatics contain compounds with two to over four aromatic rings as monoaromatic or polyaromatic (*i.e.*, polycyclic aromatic hydrocarbons, PAHs), potentially incorporating heteroatoms such as sulfur, nitrogen and oxygen.[1,10]

Resins and asphaltenes represent the most polar and intricate components of petroleum, with hydrocarbon backbones composed of naphthenic, aromatic, and heteroaromatic rings,

[a]*Department of Chemical & Petroleum Engineering, Schulich School of Engineering, University of Calgary, Calgary, Alberta T2N 1N4, Canada.*
E-mail: hhassanz@ucalgary.ca
[b]*Department of Electrical and Software Engineering, Schulich School of Engineering, University of Calgary, Alberta T2N 1N4, Canada. E-mail: zahra.abbasi@ucalgary.ca*

along with alkyl side chains. It is rather challenging to distinguish a clear border between resins and asphaltenes due to their overlapping structural characteristics.[11,12] However, resins are characterized as soluble in light alkanes (*e.g.*, pentane and heptane) but insoluble in liquid propane, while asphaltenes are soluble in aromatic hydrocarbons (benzene and toluene) and insoluble in excess amounts of light alkanes (*i.e.*, *n*-C_5–C_7).[11–13] The primary trace elements found in resins and asphaltenes are nickel and vanadium, which are concentrated in metal porphyrin complexes.[14–16]

The molecular structure models for SARA fractions have been presented in the literature. The molecular structure of asphaltenes is often described using two contrasting models: the condensed (island) structure and the dispersed (archipelago) structure. In the island model, an asphaltene molecule features a central aromatic core with many fused rings (typically more than seven rings) surrounded by aliphatic groups. In the archipelago model, asphaltenes consist of smaller aromatic units interconnected by aliphatic bridges.[7,11,12,17,18]

Adams *et al.* used model compounds to establish some chemical boundaries for the eight fractions of the SAR-AD™ characterization method for heavy oils.[10] It was found that saturates primarily consist of linear alkanes such as the model compound *n*-C_{22}, polywax, and natural waxes. Additionally, they identified 5-α-cholestane, a highly cyclic alkane, as a model compound for the saturate fraction. They classified the aromatic fraction into three categories: aro-1 fraction, with a single aromatic ring (*e.g.*, dodecylbenzene); aro-2 fraction, comprising molecules with two to three fused aromatic rings (*e.g.*, naphthalene, acenaphthylene, anthracene, and pyrene); and aro-3 fraction, consisting of larger molecules including *peri* condensed aromatics and polycyclic aromatic hydrocarbons (*e.g.*, chrysene, perylene, and coronene). Various model compound molecules were reported for the resin fraction, such as 9-hydroxyanthracene, 1-hydroxypyrene, nonylphenol, all containing a phenolic OH functional group, 9-anthracenemethanol, with a hydroxymethyl CH_2–OH functional group, and 1,10-phenanthroline, with two pyridine nitrogen atoms. The model compounds for the asphaltene subfractions were reported as *N*,*N*-bis-2-ethylhexyl-3,4,9,10-perylenetetracarboxylic diimide, coumarin 343, acenaphthenequinone, *N*,*N*-ditridecyl-3,4,9,10-perylenetetracarboxylic diimide, with polar carbonyl groups, and the charged Reichardt's dye. Although these molecules are not ideal models for SARA fractions, they provide some insight into the boundaries of these fractions.[10]

Zhang *et al.*[19,20] conducted molecular simulations to create model asphalt mixtures similar to those found in real asphalt. In their initial studies, they used *n*-C_{22} and 1,7-dimethyl naphthalene to represent saturates and naphthene aromatics, respectively. In later studies, they excluded *n*-alkanes from the saturate fraction and instead selected squalane and hopane molecules to represent the saturate fraction.[21]

Huynh *et al.* used six model aromatic compounds commonly found in crude oil, including ethylbenzene, naphthalene, biphenyl, phenanthrene, 1-benzylnaphthalene, and chrysene, to optimize off-line LC-GC-MS separation. This demonstrated that these aromatic compounds could mimic the chromatographic behavior of the aromatic fraction in petroleum samples.[22] Sundberg and Feilberg used *n*-hexadecane, toluene, naphthalene and phenanthrene as models for saturated hydrocarbons, mono-, di- and tri-aromatics, respectively, to calibrate their HPLC system for quantitative SARA-analysis.[23]

The molecular structure models for SARA fractions reported in the literature use various model compounds and structures to represent the same fraction.[4,24–29] Hence, no single component universally represents each constituent of SARA fractions. The simulated fraction models and their associated compounds and structures provide only a theoretical representation of the SARA fractions, which are primarily applicable to simulation-based studies. Since all proposed structures are only approximate models, determining reliable compounds with specific molecular structures that represent SARA fractions is highly demanded.

In this study, the actual compounds for the saturate, aromatic, resin and asphaltene fractions were identified and introduced. In the initial step, several chemicals were screened and analyzed using the SARA-HPLC chromatographic technique developed in our previous work.[30] The SARA-HPLC system is equipped with four columns: a PLgel MIXED guard and polytetrafluoroethylene (PTFE) columns for separation of asphaltenes, and ZORBAX RX-SIL- and ZORBAX CN-packed columns for separation of aromatics and resins, respectively. The saturate fraction, which does not interact with these stationary phases, is directed to the refractive index detector (RID) for quantification. In the next step, representative chemicals for each fraction were identified based on their solubility and adsorption on the corresponding columns relative to each fraction. Eventually, calibration curves for each fraction were generated using the proposed standard samples.

2. Experimental section

2.1. Materials and methods

Various chemicals were analyzed using the SARA-HPLC system to identify appropriate representative compounds for the SARA fractions. All the chemicals were purchased from Sigma-Aldrich, Thermo Fisher Scientific and TCI Chemicals. The solvents used for the experiments were HPLC grade solvents, *n*-pentane (CAS: 109-66-0), and toluene (CAS: 108-88-3), sourced from VWR Ltd. SARA-HPLC columns including the PLgel MIXED guard column (PL 1110-1320), ZORBAX CN (P.N. 880952-705), and ZORBAX RX-SIL (P.N. 880975-901) were provided by Agilent Technologies, Inc.

2.2. SARA-HPLC chromatography method

In this method, a 50 μL oil sample (diluted in toluene) is introduced into a system consisting of four columns with specific stationary phases. Initially, asphaltenes precipitate in the PLgel MIXED guard and polytetrafluoroethylene (PTFE) columns in an excess volume of *n*-pentane. The pentane-soluble maltene then passes through the ZORBAX CN and

ZORBAX RX-SIL columns. Highly polar resins are adsorbed onto the ZORBAX CN column, while moderately polar aromatics are retained on the ZORBAX RX-SIL column. The saturate fraction, which is not retained on the columns, is directed to the refractive index detector (RID) (Agilent 1200 infinity series-G7162A) for quantification. Following the separation process, aromatics, resins, and asphaltenes are eluted from their respective columns using toluene and sent to a UV-vis absorbance detector (Agilent 1290 HPLC) for quantification. UV-vis optical absorbance data are recorded at 300 nm based on the UV-vis spectra of each fraction,[30] shown in Fig. 1. More details about the SARA-HPLC technique can be found in our previous work.[30] The UV-vis spectra of aromatics, resins and asphaltenes in toluene were recorded using a VWR UV-1600PC spectrophotometer, revealing a strong peak at ~300 nm, corresponding to the n–π* transition of unsaturated bonds. Additionally, a peak at 410 nm is observed in the spectra of resins and asphaltenes, attributed to the presence of metal porphyrins, including vanadyl porphyrins.[31]

This technique overcomes the challenges of traditional separation methods, such as consuming large quantities of crude oil and solvents, complex operation, long testing periods, incomplete separation, and poor repeatability, while meeting the requirements for high-efficiency and repeatable fraction acquisition.[30]

Various chemicals were screened and analyzed using the SARA-HPLC technique to identify suitable representatives for the SARA fractions. The selection process was guided by specific criteria: all chemicals must be soluble in toluene as required by the SARA-HPLC method (where samples are diluted in toluene), representative chemicals for resin, aromatic and asphaltene fractions must adsorb exclusively to their corresponding columns, and the chemicals must exhibit a UV-vis absorbance peak at 300 nm, consistent with the properties of aromatics, resins, and asphaltenes extracted from real petroleum fluids. The subsequent sections provide a detailed explanation of the chemical selection and evaluation process.

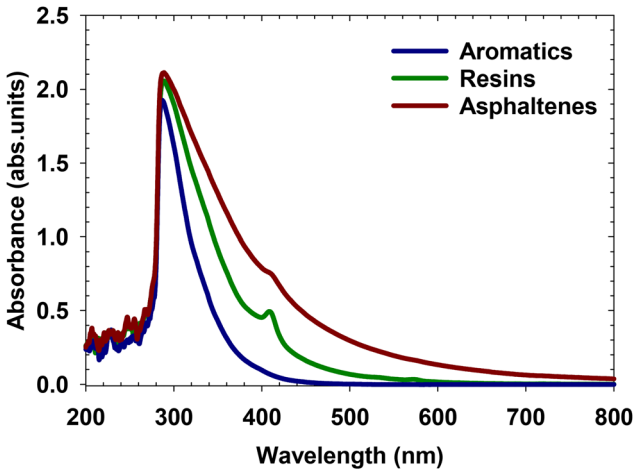

Fig. 1 UV-vis spectra of aromatics, resins, and asphaltenes with strong peaks at ~300 nm.

2.3. Representative chemicals for saturates

As mentioned earlier, the nonpolar saturate fraction is not retained and adsorbed by four chromatography columns of the SARA-HPLC system. It is directed to the RID for measurement due to its minimal interaction with the column's stationary phases. Since the injected sample to the SARA-HPLC system should be diluted in toluene, the solubility of several *n*-alkanes in toluene was assessed from *n*-C_6 to *n*-C_{60}. It was found that *n*-alkanes from *n*-C_6 to *n*-C_{36} were soluble in toluene, which could be considered for the saturate fraction. It should be mentioned that polywax 655, a mixture of *n*-C_{20} to *n*-C_{100} with a complex structure, was found to be insoluble in toluene.

2.4. Representative chemicals for aromatics

The representative compounds for the aromatic fraction must adsorb onto the highly active silica gel stationary phase (ZORBAX RX-SIL column of the SARA-HPLC system) while exhibiting a UV-vis absorbance peak at 300 nm. Based on the molecular structure of the aromatic fraction discussed earlier, simple aromatic molecules with 2- and 3-fused rings, as well as the 4-ring molecule pyrene, were initially evaluated. As a result, fluorene, 9,10-dihydrophenanthrene, anthracene, phenanthrene, fluoranthene, 2-ethylanthracene, and pyrene were identified as suitable candidates, shown in Fig. 2, as they adsorbed exclusively onto the ZORBAX RX-SIL column and aligned with the expected characteristics of the aromatic fraction (*i.e.*, exhibiting a UV-vis absorbance peak at 300 nm).

The aromatic fraction may also contain a small number of heteroatoms, including nitrogen (N), oxygen (O), and sulfur (S). However, highly polar functional groups (*e.g.*, phenols, carboxylic acids, esters, or thiols) are not typically expected. Therefore, simple heteroatomic aromatic compounds, such as nitrobenzene, dibenzofuran, dibenzothiophene, and 4-methyldibenzothiophene, were assessed. Among these chemicals, only nitrobenzene demonstrated the proper characteristics of the aromatic fraction, while dibenzofuran, dibenzothiophene, and 4-methyldibenzothiophene did not exhibit a peak at 300 nm wavelength. Fig. 2 illustrates the molecular structures of the appropriate chemicals for the aromatic fraction.

Additionally, larger aromatic molecules with 4- and 5-fused rings, such as perylene, benzo(e)pyrene, benzo(ghi)perylene, and 7,12-dimethylbenz(α)anthracene, suggested by Adams *et al.*,[10] were evaluated. Perylene displayed a UV-vis absorbance peak at 430 nm, which falls outside the specified wavelength of the SARA-HPLC system for the aromatic fraction. Furthermore, benzo(e)pyrene, benzo(ghi)perylene, and 7,12-dimethylbenz(α)anthracene exhibited peaks for aromatic, resin, and asphaltene fractions, indicating adsorption onto multiple columns (ZORBAX CN and ZORBAX RX-SIL) and precipitation in the PTFE column.

2.5. Representative chemicals for resins

Due to the overlapping structural characteristics of resins and asphaltenes, it is highly challenging to distinguish a clear border between resins and asphaltenes. Resins exhibit a com-

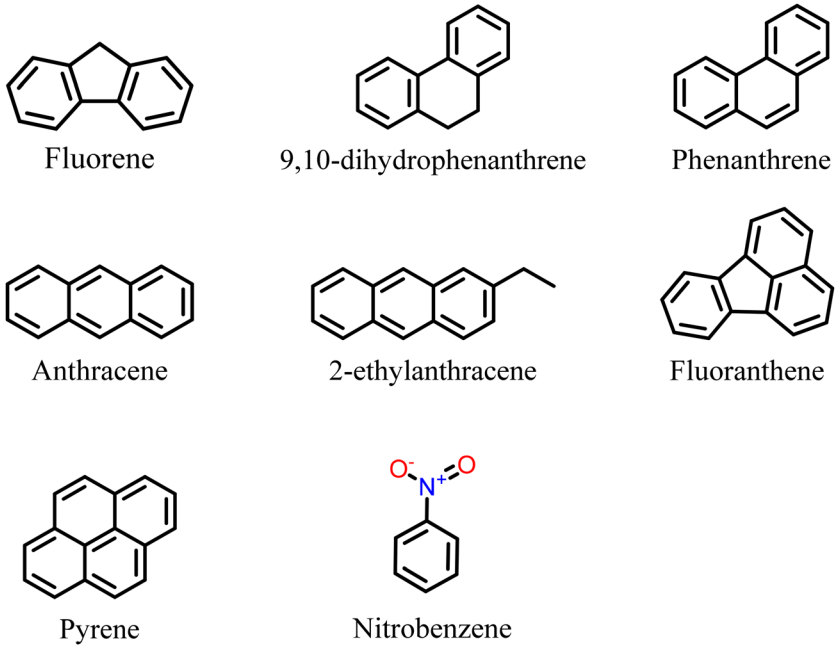

Fig. 2 Molecular structures of the appropriate chemicals for the aromatic fraction. The functional group $-NO_2$ is designated for the nitro group.

bination of polar and nonpolar functional groups, acting as intermediates that link low-polarity aromatic compounds to highly polar asphaltenes. Consequently, resins are expected to possess molecular structures resembling aromatics but with additional polar functional groups. The incorporation of polar carbonyl (C═O) and hydroxymethyl ($-CH_2OH$) groups into the fused-ring aromatic structure of anthracene introduces moderate polarity and reactivity, yielding molecules that bridge the characteristics of aromatics and asphaltenes. 9-Anthracenemethanol and anthrone are the resulting molecules representing the resin characteristics, shown in Fig. 3.

2.6. Representative chemicals for asphaltenes

Asphaltene compounds must be insoluble in pentane, the carrier phase, to ensure precipitation in the first column (guard and PTFE columns) of the SARA-HPLC system. Due to the large molecular size, complex structures, and diverse functional group characteristics of asphaltenes, a variety of chemicals were screened. Initially, compounds with large molecular frameworks containing heteroatoms, like the island architecture model of asphaltenes, were tested to replicate the appearance and properties of asphaltenes. *N*,*N*-Ditridecyl-3,4,9,10-perylenetetracarboxylic diimide and perylene-3,4,9,10-tetracarboxylic dianhydride, featuring a perylene aromatic core with four carbonyl groups and two anhydride groups, respectively, were tested and found to be insoluble in toluene. This insolubility is attributed to the highly polar functional groups, which promote strong intermolecular interactions such as hydrogen bonding and dipole–dipole interactions, leading to aggregation in moderately polar solvents like toluene.

After the failure of toluene solubility for chemicals with a large molecular structure and high polarity, the approach shifted to using smaller and less polar molecules. 2,3-Dihydroxybenzoic and 1,4-dihydroxy-2-naphthoic acid, consisting of two hydroxyl groups and one carboxylic acid group with one and two aromatic rings, respectively, were insoluble in toluene. Apparently, their polar functional groups form strong hydrogen bonds, resulting in less interaction with toluene.

It is essential to balance molecular size, polarity, and aromaticity to obtain suitable asphaltene compounds. Consequently, compounds such as salicylic acid, 1,10-phenanthroline, *m*-nitrophenol, 2,2′-bipyridine, 1-hydroxy-2-naphthoic acid, fluorene-9-carboxylic acid, and bathophenanthroline were found to be soluble in toluene but insoluble in pentane. These compounds precipitate in the guard and PTFE columns of the SARA-HPLC system, exhibiting a UV-vis absorbance peak at 300 nm, which aligns with the typical properties of the asphaltene fraction. All these chemicals are characterized by smaller molecular sizes of 1 to 4 aromatic rings compared to larger molecules of asphaltenes reported in the literature with polar functional groups, including hydroxyl (–OH), carbonyl (–COOH), and nitro ($-NO_2$) groups. Additionally, 1,10-phenan-

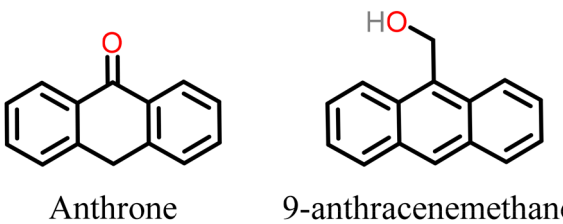

Fig. 3 Molecular structures of the appropriate chemicals for the resin fraction. The functional groups $-CH_2-OH$ and C═O are designated for the hydroxymethyl and carbonyl groups, respectively.

throline, 2,2′-bipyridine, and bathophenanthroline contain two pyridine nitrogen groups within their molecular structures. The polarity of these functional groups enables the compounds to dissolve in toluene, a relatively polar solvent, while being insoluble in nonpolar solvents like pentane. Fig. 4 shows the molecular structures of the proposed chemicals for asphaltenes.

It should be noted that two asphaltene model compounds suggested by Adams *et al.*[10] were evaluated individually by loading each sample into the SARA-HPLC system. Acenaphthenequinone was found to generate two peaks in the resin and asphaltene fractions, indicating partial adsorption onto the resin column. Furthermore, coumarin 343 exhibited very poor solubility in toluene. As a result, injecting a highly diluted sample into toluene failed to generate a peak for the asphaltene fraction.

3. Results and discussion

The current section provides a detailed description of the method used to identify standard fractions of SARA. To evaluate the behavior of the proposed standard samples for each fraction, SARA fractionation was performed on an actual crude oil sample with a molecular weight of 513.3 g mol^{-1}, an API gravity of 9.43, and a viscosity of 14 022 cP (at 45 °C and 1.12 MPa).[32] The molecular weight and API gravity were measured using vapor pressure osmometry (VPO, Gonotec-Osmomat 070) and an Anton Paar DMA 5000 M digital oscillating U-tube densitometer, respectively. The SARA separation was carried out using two preparative chromatography columns packed with cyano and silica gel stationary phases. The process began by separating the asphaltene content from the crude oil sample using *n*-pentane solvent, following the ASTM D2007 standard method. Then, the de-asphalted mixture (maltene) in *n*-pentane was passed through the cyano and silica columns to separate the resin and aromatic fractions, respectively. The saturate fraction, which does not adsorb to these columns, was collected directly in a flask. In the last step, toluene, as the mobile phase, was used to wash out each fraction from the respective columns. These steps and operational conditions closely resemble the developed SARA-HPLC protocol, which effectively addresses and mitigates the issue of cross-contamination in fractions. The resulting SARA data and properties of the crude oil sample are summarized in Table 1. The four separated fractions were used in subsequent steps to evaluate the standard SARA samples.

3.1. Standard saturate sample

The extracted saturate fraction from the crude oil was diluted in toluene with a concentration of 0.0013 g ml^{-1} and then injected into the SARA-HPLC system, which yielded a peak area of 153 421 nRIU recorded using the RID. The selected concentration (0.0013 g ml^{-1}) is in the optimized concentration range of the SARA-HPLC system shown in our previous work.[30] Since identifying a single component matching this peak area (153 421 nRIU) at the same concentration (0.0013 g ml^{-1}) is impractical, a mixture of saturate samples mentioned

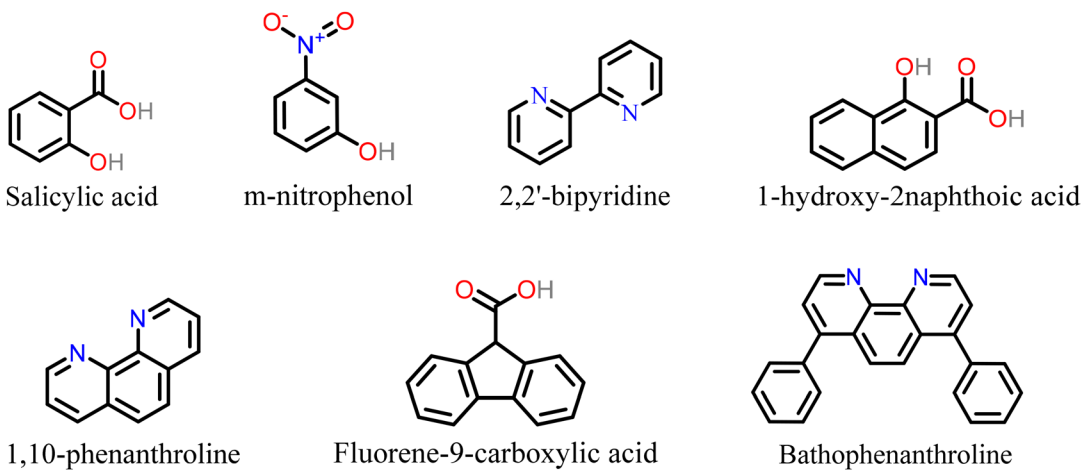

Fig. 4 Molecular structures of the proposed chemicals for asphaltenes. The functional polar groups consist of –OH (hydroxyl group), –COOH (carboxylic group), –N (nitrogen atom), and $-NO_2$ (nitro group).

Table 1 Properties of the crude oil sample

SARA fractionation (wt%)						
Saturates	Aromatics	Resins	Asphaltenes	Molecular weight (g mol^{-1})	Viscosity[32] (cP), at 45 °C and 1.12 MPa	API at 15 °C
27.80	36.90	15.80	19.50	513.30	14 022	9.43

in the previous section needs to be considered. Therefore, each *n*-alkane of *n*-C_6 to *n*-C_{36} was individually loaded into the SARA-HPLC system at a concentration of 0.0013 g ml^{-1}, and the corresponding peak areas were recorded. For simplicity, two representative *n*-alkanes with lower and upper peak areas compared to 153 421 nRIU were selected: *n*-C_6, with a peak area of 78 772 nRIU, and *n*-C_{36} with a peak area of 306 443 nRIU, bracketing the target value of 153 421 nRIU.

In the next step, to determine the optimal ratio of these two chemicals, mixtures at varying ratios at the concentration of 0.0013 g ml^{-1} in toluene were prepared and loaded into the system, as shown in Fig. 5a. The optimum ratio of the *n*-C_6 and *n*-C_{36} mixture was determined by matching the target peak area of 153 421 nRIU using Fig. 5a, resulting in a 33% *n*-C_{36} and 67% *n*-C_6 composition as the proposed standard saturate sample. A calibration curve was subsequently generated with different concentrations of the standard saturate sample, presented in Fig. 5b, that is completely matched and aligned with the one obtained from the saturate fraction of crude oil.

3.2. Standard aromatic sample

The separated aromatic fraction of crude oil, with a concentration of 0.002 g ml^{-1} in toluene, was prepared and injected into the SARA-HPLC system, yielding a peak area of 27 765 mAU min as recorded using the UV-vis detector. The selected concentration of 0.002 g mL^{-1} falls within the optimized concentration range for the aromatic fraction in the SARA-HPLC system, as demonstrated in our previous work.[30] Since it is impractical to identify a single chemical that matches this peak area at the same concentration, a mixture of two aromatic compounds was considered. The suitable aromatic chemicals, identified earlier in the Experimental section, were individually analyzed using the SARA-HPLC system at a concentration of 0.002 g ml^{-1}, and their respective peak areas were recorded. Among these chemicals, phenanthrene (8258 mAU min) and nitrobenzene (39 094 mAU min) were selected as they bracketed the target peak area of 27 765 mAU min. Fig. 6 presents phenanthrene and nitrobenzene chromatograms (UV-vis detector responses), demonstrating that these compounds exclusively adsorb onto the ZORBAX RX-SIL packed column. Notably, they exhibit no adsorption or affinity for other columns, which is favorable for SARA fractionation.

After identifying two appropriate chemicals representing the aromatic fraction, various phenanthrene and nitrobenzene mixtures were prepared in toluene and analyzed to determine the optimal ratio, as shown in Fig. 7a. The results indicated that a mixture of 65% nitrobenzene and 35% phenanthrene provided the best match to the target peak area of the aromatic fraction (27 765 mAU min), establishing this combination as the proposed standard aromatic sample. A calibration curve was subsequently created using different concentrations of this standard mixture, presented in Fig. 7b, which closely aligned with the calibration curve obtained from the aromatic fraction of crude oil.

3.3. Standard resin sample

The resin fraction was diluted in toluene with a concentration of 0.00168 g ml^{-1} and then was loaded into the SARA-HPLC system, giving a peak area of 36 952 mAU min. The selected concentration of 0.00168 g mL^{-1} falls within the optimized concentration range for the resin fraction in the SARA-HPLC system, as reported in our previous work.[30] Since this peak area could not be replicated by a single compound, a mixture of 9-anthracenemethanol, with a peak area of 4041 mAU min, and anthrone, with a peak area of 49 582 mAU min, was considered as their corresponding peak areas bracketed the target peak area (36 952 mAU min). Fig. 8 shows the UV-vis chromatograms of both compounds, confirming the exclusive adsorption of these chemicals onto the ZORBAX CN-packed column, similar to the actual resin fraction of the petroleum mixture.

To determine the optimal ratio, mixtures of 9-anthracenemethanol and anthrone in toluene were prepared at a fixed concentration of 0.00168 g ml^{-1} and analyzed for peak areas, as shown in Fig. 9a. The best match to the resin faction target

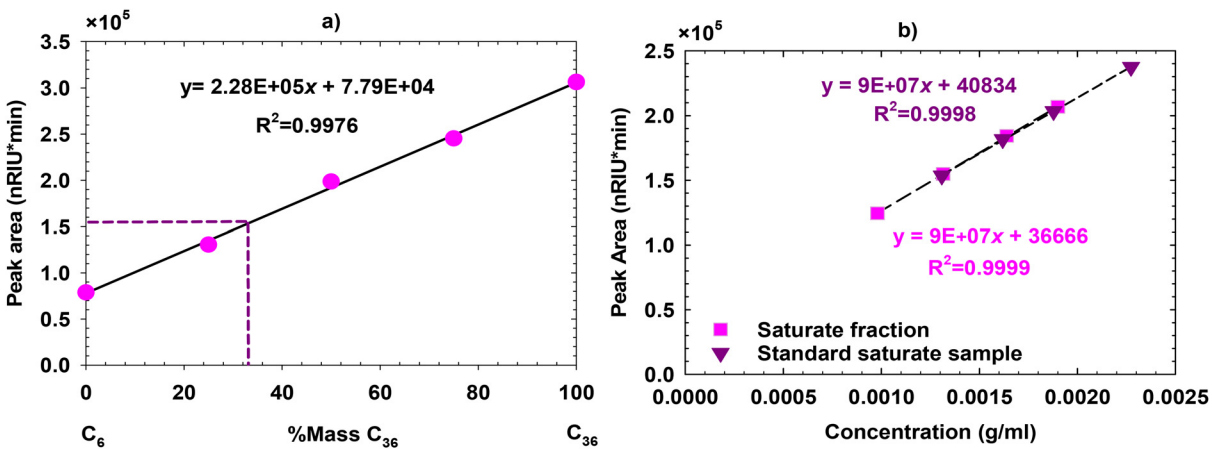

Fig. 5 (a) Different ratios of the *n*-C_6 and *n*-C_{36} mixture at a concentration of 0.0013 g ml^{-1} and the corresponding peak area. (b) Calibration curves for the saturate fraction, shown with light pink squares, and the standard saturate sample, shown with dark pink triangles.

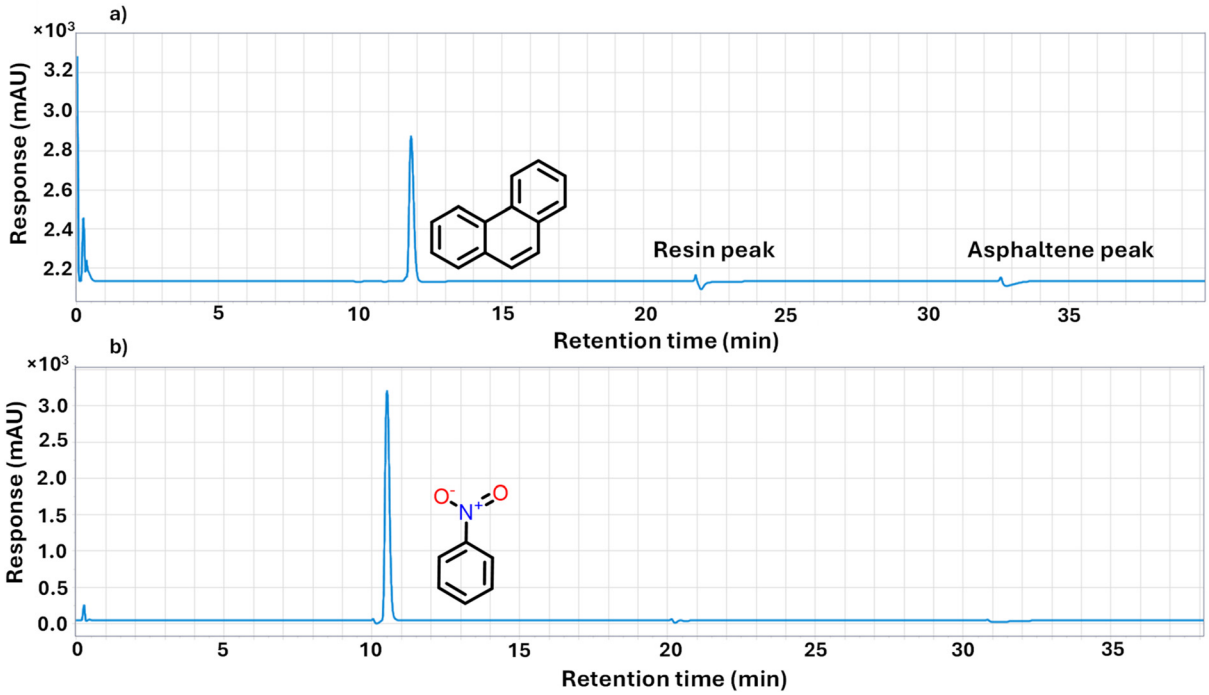

Fig. 6 UV-vis response for the proposed standard aromatic sample: (a) phenanthrene and (b) nitrobenzene. Both compounds adsorb onto the ZORBAX RX-SIL packed column, while there is no adsorption or affinity for other columns.

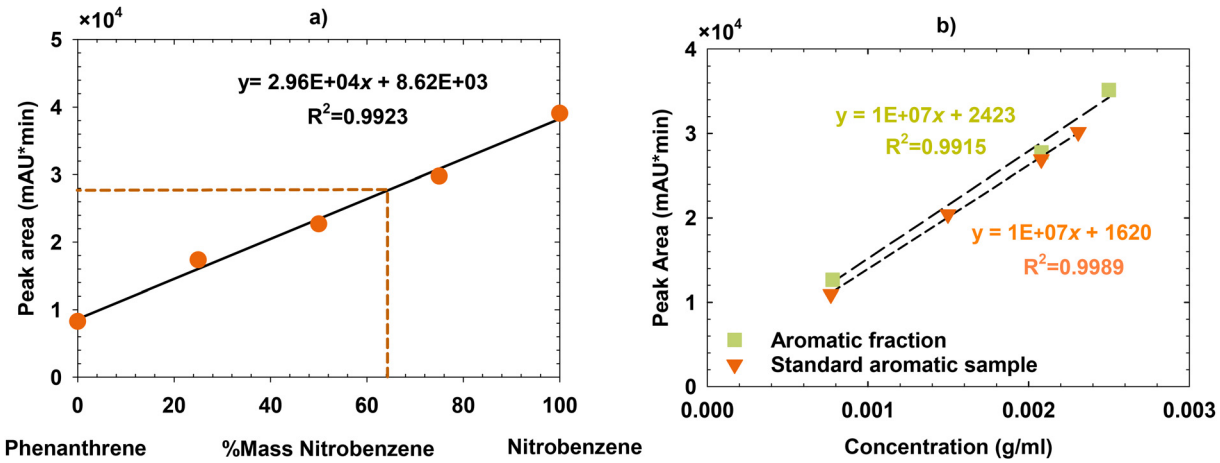

Fig. 7 (a) Different ratios of the phenanthrene and nitrobenzene mixture at a concentration of 0.002 g ml^{-1} and the corresponding peak area. (b) Calibration curves for the aromatic fraction, shown by dark yellow squares, and the standard aromatic sample, shown by orange triangles.

peak area (36 952 mAU min) was achieved with a mixture of 71% anthrone and 29% 9-anthracenemethanol, designating this combination as the standard resin fraction, Fig. 9a. In the last step, a calibration curve was generated using various concentrations of this standard mixture, illustrated in Fig. 9b, which perfectly matched the resin fraction's calibration curve.

3.4. Standard asphaltene sample

Following the similar procedure of other fractions, the asphaltene fraction was diluted to a concentration of 0.00170 g ml^{-1} in toluene and loaded to the SARA-HPLC system, which gives a peak area of 95 256 mAU min. The selected concentration of 0.00170 g mL^{-1} falls within the optimized concentration range for the asphaltene fraction in the SARA-HPLC system shown in our previous work.[30] Then, a combination of salicylic acid, with a peak area of 65 901 mAU min, and bathophenanthroline, with a peak area of 141 285 mAU min, was evaluated, as their individual peak areas encompassed the target value of 95 256 mAU min, as shown in Fig. 10. According to Fig. 10, there is no peak for the aromatic and resin fractions, indicat-

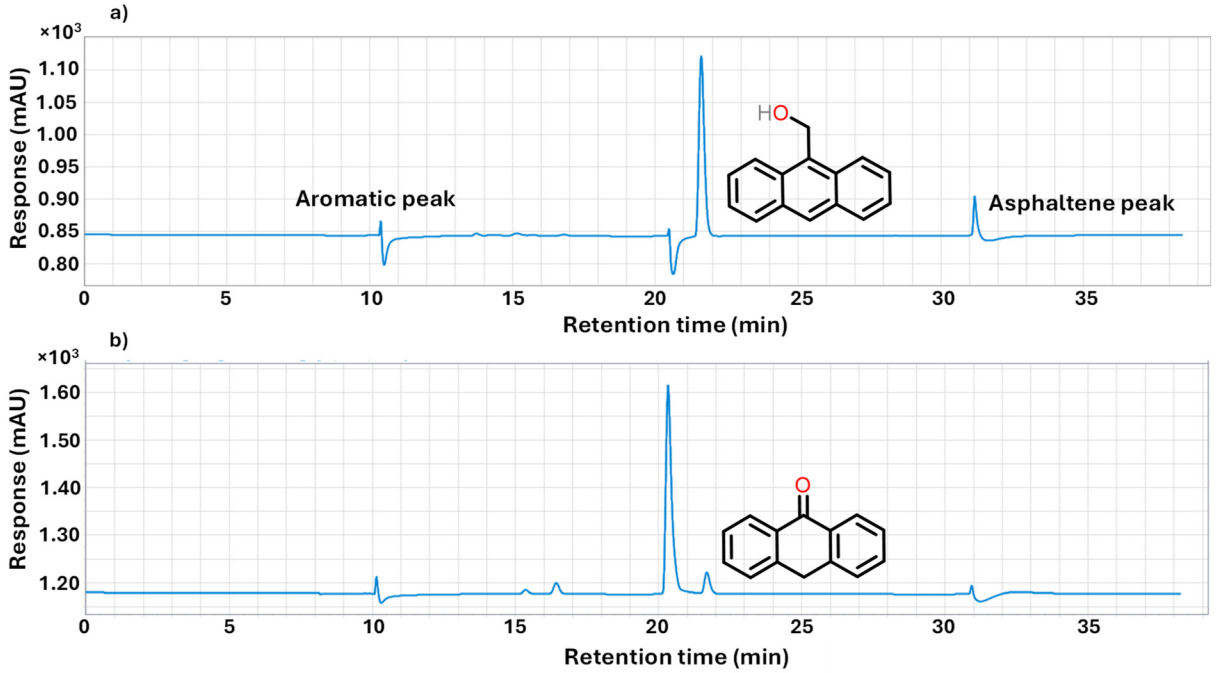

Fig. 8 UV-vis response for the proposed standard resin samples: (a) 9-anthracenemethanol and (b) anthrone. Both compounds adsorb onto the ZORBAX CN packed column, while there is no adsorption or affinity for other columns.

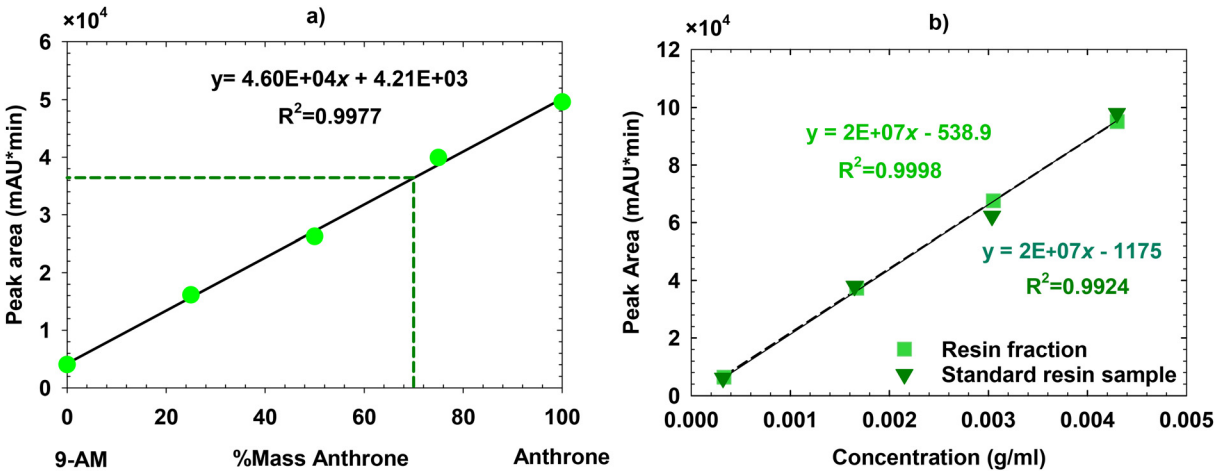

Fig. 9 (a) Different ratios of the 9-anthracenemethanol (9-AM) and anthrone mixture at a concentration of 0.00168 g ml^{-1} and the corresponding peak area. (b) Calibration curves for the resin fraction, shown by light green squares, and the standard resin sample, shown by dark green triangles.

ing that both compounds precipitate in the guard and PTFE columns of the SARA-HPLC system, with no adsorption or affinity for other columns.

In the following step, salicylic acid and bathophenanthroline mixtures were analyzed at a fixed concentration of 0.00170 g ml^{-1}, as illustrated in Fig. 11a. The best match to the target peak area of the asphaltene fraction (95 256 mAU min) was achieved using a mixture containing 38% bathophenanthroline and 62% salicylic acid, as shown in Fig. 11a, which was selected as the standard asphaltene fraction sample. A calibration curve was then generated using different concentrations of this mixture, shown in Fig. 11b, which closely matched the calibration curve for the asphaltene fraction.

It should be noted that the selection of concentration ranges for each SARA fraction was guided by two primary considerations: the group-type composition of a crude oil sample (mentioned in Table 1), as determined through SARA analysis (ASTM D2007), and the fixed oil concentration of 0.006 g mL^{-1} required for operation of the SARA-HPLC system.[30] Using the weight percent composition of each fraction, the corresponding concentration (in g ml^{-1}) at this dilution was calcu-

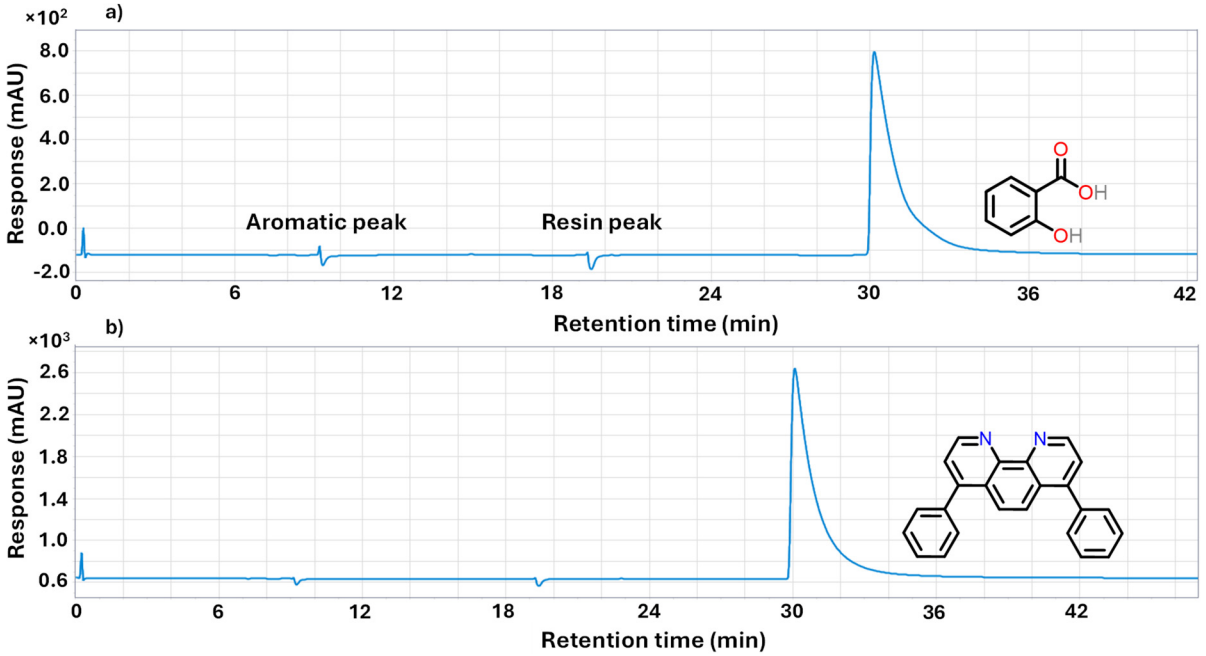

Fig. 10 UV-vis response for the proposed standard asphaltene samples: (a) salicylic acid and (b) bathophenanthroline. Both compounds precipitate in the guard and columns, while there is no adsorption or affinity for the other columns.

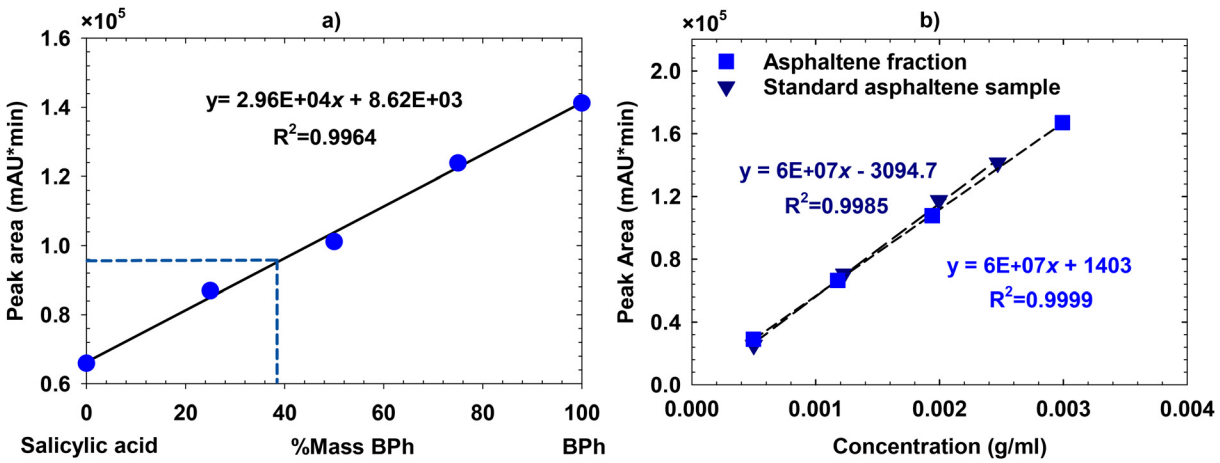

Fig. 11 (a) Different ratios of the salicylic acid and bathophenanthroline (BPh) mixture at a concentration of 0.00170 g ml^{-1} and the corresponding peak area. (b) Calibration curves for the asphaltene fraction, shown by blue squares, and the standard asphaltene sample, shown by dark blue triangles.

lated. Then, the lower and upper limits of these calculated values were extended to ensure coverage of potential variability across different crude oil types and to provide robust calibration for samples with lower or higher group-type contents.

According to the generated calibration curves (Fig. 5, 7, 9, and 11), a strong linear relationship exists between chromatogram peak areas and concentrations of various fractions, indicating the linearity of the detector response. The new calibration curves of the proposed SARA standard samples are completely matched and aligned with those of each SARA fraction, indicating their reliability and accurate representation of their respective fractions. More importantly, the proposed compounds for each fraction adsorbed solely onto their corresponding columns, with no adsorption or affinity for other columns, which is desirable in the SARA separation procedure.

Following the aforementioned validation of the new calibration curves, the SARA-HPLC system and the new calibration curves were used to fractionate a set of ten crude oil samples with varying API gravities, ranging from bitumen and heavy oils to light oils. The results are summarized in Table 2. The

Table 2 SARA analysis of different crude oil samples

Oil sample	API at 15 °C	SARA fractionation (wt%)			
		Saturates	Aromatics	Resins	Asphaltenes
1	7.09	28.30	39.10	11.40	21.20
2	8.01	22.51	40.17	16.41	20.25
3	9.43	27.28	38.52	15.30	19.20
4	10.42	24.82	40.98	17.93	16.27
5	16.97	34.19	36.27	12.91	16.64
6	25.30	36.71	39.08	12.01	12.19
7	33.46	78.68	15.01	3.59	2.71
8	34.23	67.33	26.48	3.29	2.90
9	34.38	73.73	15.69	4.36	6.21
10	43.75	94.77	3.42	0.82	0.98

sample set covered a wide range of SARA fractions: 22.51–94.77 wt% saturates, 3.42–40.98 wt% aromatics, 0.82–17.93 wt% resins, and 0.98–21.20 wt% asphaltenes. As a result, the SARA-HPLC system, along with the proposed SARA standard samples and the generated calibration curves, appears to be broadly applicable across diverse crude oil and bitumen samples.

Sample 3 is the oil sample that was fractionated using two preparative liquid adsorption chromatography columns packed with cyano and silica gel according to ASTM D2007. This sample was used to evaluate the behavior of the proposed standard compounds for each SARA fraction, described in the Results and discussion section. According to Tables 1 and 2, all the measured fractions of Sample 3 obtained using the gravimetric adsorption open-column chromatography method are comparable to those measured using the SARA-HPLC system with the new SARA calibrations based on the proposed standard samples, showing a standard deviation of 0.36, 1.14, 0.35, and 0.21wt% for saturates, aromatics, resins and asphaltenes, respectively.

The proposed SARA standard samples offer a practical calibration strategy for laboratories utilizing the SARA-HPLC system, particularly where the direct fractionation and isolation of individual SARA fractions from crude oil are labor-intensive, time-consuming, or not feasible. By using the proposed standard compounds, the SARA-HPLC system can be calibrated quickly and reproducibly, eliminating the need for fresh calibration with every crude oil or bitumen sample.

4. Conclusions

This study identified and characterized the representative standard samples for the saturate, aromatic, resin, and asphaltene fractions using the SARA-HPLC technique. The proposed saturate standard consists of a mixture of 67% *n*-C_6 and 33% *n*-C_{36}, while the aromatic standard comprises 65% nitrobenzene and 35% phenanthrene. The resin standard is composed of 71% anthrone and 29% 9-anthracenemethanol, and the asphaltene standard is a mixture of 62% salicylic acid and 38% bathophenanthroline. The proposed standard samples for asphaltenes exhibit complete precipitation in the guard and PTFE columns, like the real petroleum asphaltene fraction, without affinity or adsorption onto other columns. Similarly, the aromatic and resin standard samples adsorb solely onto their respective columns, ZORBAX RX-SIL and ZORBAX CN. These proposed standard samples align with the behavior of the actual SARA fractions of petroleum mixtures, demonstrating their accuracy and reliability as representative standards. By introducing these new standard SARA samples, the SARA-HPLC technique is being further standardized and calibrated, potentially reducing the reliance on calibration with actual petroleum individual SARA fractions. These new standard SARA samples address the limitation of SARA fractionation methods by removing the repeatability challenges and the time-consuming and cumbersome calibration procedures.

Author contributions

Shadi Kheirollahi: conceptualization, data curation, formal analysis, investigation, methodology, validation, visualization, writing – original draft, and writing – review and editing. Mabkhot Bin Dahbag: conceptualization, formal analysis, data curation, investigation, validation, methodology, supervision, and writing – review and editing. Zahra Abbasi: conceptualization, formal analysis, funding acquisition, investigation, methodology, project administration, resources, supervision, validation, and writing – review and editing. Hassan Hassanzadeh: conceptualization, formal analysis, funding acquisition, investigation, methodology, project administration, resources, supervision, validation, and writing – review and editing.

Conflicts of interest

There are no conflicts to declare.

Data availability

Data will be made available from the corresponding author upon reasonable request.

Acknowledgements

The authors acknowledge the financial support from the Natural Sciences and Engineering Research Council of Canada (NSERC) and all member companies of the SHARP Research Consortium: Canadian Natural Resources Limited (CNRL), Cenovus Energy, Imperial Oil Limited, Kuwait Oil Company, Strathcona Resources, and Suncor Energy. In addition, the support of the Department of Chemical and Petroleum Engineering and the Schulich School of Engineering at the University of Calgary is highly appreciated.

References

1 E. B. Overton, T. L. Wade, J. R. Radović, B. M. Meyer, M. S. Miles and S. R. Larter, *Oceanography*, 2016, **29**, 50–63.
2 E. B. Overton, D. L. Wetzel and J. K. Wickliffe, *Scenarios and Responses to Future Deep Oil Spills*, Springer, Cham, 2020, ch. 3, pp. 33–56. DOI: **10.1007/978-3-030-12963-7**.
3 L. Szepesy, *Trends Anal. Chem.*, 1985, **4**, 258–261.
4 M. Guo, M. Liang, Y. Fu, A. Sreeram and A. Bhasin, *Mater. Struct. Constr.*, 2021, **54**(4), 173, DOI: **10.1617/s11527-021-01754-2**.
5 I. A. Wiehe and K. S. Liang, *Fluid Phase Equilib.*, 1996, **117**, 201–210.
6 I. Shishkova, D. Stratiev, I. V. Kolev, S. Nenov, D. Nedanovski, K. Atanassov, V. Ivanov and S. Ribagin, *Energies*, 2022, **15**(20), 7765, DOI: **10.3390/en15207765**.
7 K. Primerano, J. Mirwald and B. Hofko, *Fuel*, 2024, **368**, 131616.
8 B. P. Vempatapu, J. Kumar, B. Upreti and P. K. Kanaujia, *TrAC, Trends Anal. Chem.*, 2024, **177**, 117810.
9 S. Gutiérrez Sama, C. Barrère-Mangote, B. Bouyssière, P. Giusti and R. Lobinski, *TrAC, Trends Anal. Chem.*, 2018, **104**, 69–76.
10 J. J. Adams, J. F. Rovani, J. P. Planche, J. Loveridge, A. Literati, I. Shishkova, G. Palichev, I. Kolev, K. Atanassov, S. Nenov, S. Ribagin, D. Stratiev, D. Yordanov and J. Huo, *Processes*, 2023, **11**(4), 1220, DOI: **10.3390/pr11041220**.
11 T. V. Cheshkova, V. P. Sergun, E. Y. Kovalenko, N. N. Gerasimova, T. A. Sagachenko and R. S. Min, *Energy Fuels*, 2019, **33**, 7971–7982.
12 E. Y. Kovalenko, T. A. Sagachenko, K. A. Cherednichenko, N. N. Gerasimova, T. V. Cheshkova and R. S. Min, *Energy Fuels*, 2023, **37**, 8976–8987.
13 A. Demirbas and O. Taylan, *Pet. Sci. Technol.*, 2016, **34**, 771–777.
14 A. M. Mckenna, J. M. Purcell, R. P. Rodgers and A. G. Marshall, *Energy Fuels*, 2009, **23**, 2122–2128.
15 K. Qian, A. S. Mennito, K. E. Edwards and D. T. Ferrughelli, *Rapid Commun. Mass Spectrom.*, 2008, **22**(14), 2153–2160.
16 K. Qian, K. E. Edwards, A. S. Mennito, C. C. Walters and J. D. Kushnerick, *Anal. Chem.*, 2010, **82**, 413–419.
17 A. K. Tharanivasan, PhD thesis, University of Calgary, 2012.
18 S. Acevedo and J. Castillo, *ACS Omega*, 2023, **8**, 4453–4471.
19 L. Zhang and M. L. Greenfield, *Energy Fuels*, 2008, **22**, 3363–3375, DOI: **10.1021/ef700699p**.
20 L. Zhang and M. L. Greenfield, *Energy Fuels*, 2007, **21**, 1712–1716, DOI: **10.1021/ef060658j**.
21 D. D. Li and M. L. Greenfield, *Fuel*, 2014, 347–356, DOI: **10.1016/j.fuel.2013.07.012**.
22 K. Huynh, A. E. Jensen and J. Sundberg, *PeerJ Anal. Chem.*, 2021, **3**, e12.
23 J. Sundberg and K. L. Feilberg, *J. Pet. Sci. Eng.*, 2020, **184**, 106563.
24 A. Ahmed, Y. Cho, K. Giles, E. Riches, J. W. Lee, H. I. Kim, C. H. Choi, S. Kim, *et al.*, *Anal. Chem.*, 2014, **86**, 3300–3307.
25 J. M. Sheremata, M. R. Gray, H. D. Dettman and W. C. McCaffrey, *Energy Fuels*, 2004, **18**, 1377–1384.
26 M. R. Yakubov, G. R. Abilova, S. G. Yakubova and N. A. Mironov, *Pet. Chem.*, 2020, **60**, 637–647.
27 T. F. Yen, W. H. Wu and G. V. Chilingar, *Energy Sources*, 1984, **7**(3), 203–235.
28 Y. Cho, Y. H. Kim and S. Kim, *Anal. Chem.*, 2011, **83**, 6068–6073.
29 J. Murgich, J. A. Abanero and O. P. Strausz, *Energy Fuels*, 1999, **13**, 278–286.
30 S. Kheirollahi, M. BinDahbag, H. Bagherzadeh, Z. Abbasi and H. Hassanzadeh, *Fuel*, 2024, **371**, 131884.
31 I. N. Evdokimov, A. A. Fesan and A. P. Losev, *Energy Fuels*, 2017, **31**, 1370–1375.
32 M. Zirrahi, H. Hassanzadeh and J. Abedi, *Can. J. Chem. Eng.*, 2017, **95**(7), 1417–1427.